Journal of the Operations Research Society of Japan
Vol. 55, No. 2, June 2012, pp. 125–145

TOPOLOGY OPTIMIZATION OF TENSEGRITY STRUCTURES UNDER SELF-WEIGHT LOADS

Yoshihiro Kanno
University of Tokyo

(Received November 11, 2011)

Abstract A tensegrity structure is a prestressed pin-jointed structure consisting of continuously connected tensile members (cables) and disjoint compressive members (struts). This paper addresses topology optimization of tensegrity structures subjected to self-weight loads, where the compliance, i.e., the strain energy at the equilibrium state, is to be minimized. It is shown that the optimization problem can be formulated as a mixed integer linear programming (MILP) problem. The proposed method does not require connectivity relation of cables and struts of a tensegrity structure to be known in advance. Numerical experiments illustrate that various tensegrity structures can be found by solving the presented MILP problem.

Keywords: Optimization, mixed integer programming, structural optimization, tensegrity, tension structure, design-dependent constraint

1. Introduction

The terminology *tensegrity*, coined by Fuller [13] from *tension integrity*, represents a particular class of tension structures invented by Richard Buckminster Fuller [12], David Georges Emmerich [11], and Kenneth Snelson [30]. A tensegrity structure is a prestressed pin-jointed structure consisting of continuous tensile members (cables) and discontinuous compressive members (struts). An example of a tensegrity structure is shown in Figure 1. This tensegrity structure consists of three struts and nine cables connected by six nodes, where struts and cables are depicted by thick and thin lines, respectively. Here, struts do not touch each other, while cables are connected continuously. The nodes are aligned in the shape of a twisted triangular prism. By introducing an axial tensile force to each cable, this tensegrity structure attains a stable equilibrium state. The forces introduced at this initial equilibrium state are called the *prestress forces*.

Since cables of a tensegrity structure are very thin compared with struts, tensegrity structures often give the impression of a cluster of struts floating in the air. Snelson has been creating many tensegrity structures as fascinating sculptures [31] with his intuition as an artist and sophisticated techniques developed over the years. Fuller and Emmerich, in contrast, explored possibility of application of tensegrity structures to architecture. This attempt, afterward, has been realized as, e.g., tensegrity domes [25]. Following these pioneers, various methods for finding forms of tensegrity structures have been proposed by many researchers; see surveys due to Juan and Mirats Tur [20] and Tibert and Pellegrino [35]. Note that an arbitrarily given geometrical configuration is not necessarily realized as a tensegrity structure because the configuration of a tensegrity structure depends on the prestress forces. Most of the proposed numerical methods require to specify topology of a tensegrity structure as input data, where by topology we mean the connectivity of struts and cables of a tensegrity structure. Finding new topologies of tensegrity structures has been

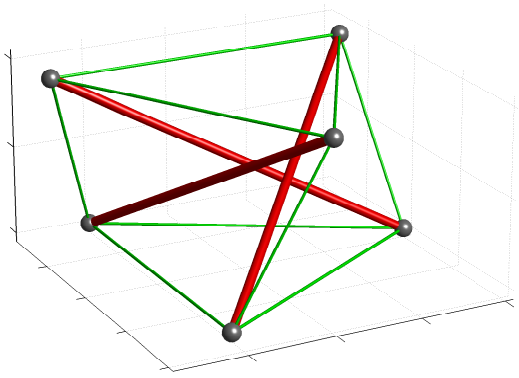

Figure 1: An example of a tensegrity structure

fully addressed only by few authors and remains as a challenging problem. For example, based on the group representation theory [8], Back and Connelly [3] attempted to enumerate tensegrity structures with the specified symmetry property. There exist only few numerical methods that can find asymmetric topology of tensegrity structures [10, 21, 26].

Today the original definition of tensegrity has been extended in various ways; see Motro [24] and the references therein. It has been recognized, or at least expected, that potential applications of tensegrity structures include architectural and civil engineering structures [1, 4, 25], deployable structures [33, 34], and cell cytoskeleton models in biomechanics [36, 37]. They are also studied in the graph theory [5, 19, 32].

On the basis of this overview, it is desired to develop numerical methods that can find various topologies of tensegrity structures without experience and intuition. The author proposed a *mixed integer linear programming* (MILP) approach to topology optimization of compliance of a tensegrity structure subjected to a fixed external load [21]. In continuation of that previous work, this paper addresses self-weight loading. The self-weight load depends on design of a structure and design is certainly unknown in the course of optimization. Therefore, topology optimization of structures with the self-weight loads possesses particular difficulties. This problem was discussed by Rozvany [27] for the plastic design, and subsequently studied for arches [28], beams and columns [2, 22, 29], composite structures [23], shell structures [18], and continua [6]. Nevertheless, the self-weight load is still often neglected in optimization of structures. However, tensegrity structures are unusual structures in the sense that stiff structural elements, i.e., struts, are not connected to each other, and hence they are relatively flexible in general. Therefore, it is important to consider the self-weight load, which might significantly affect the equilibrium configuration of a tensegrity structure. It is often that the compliance, i.e., the external work done by an applied load, is used as a measure of global flexibility of a structure. Hence, by minimizing the compliance under the self-weight load we can find a tensegrity structure which is stiff against the self-weight load.

The paper is organized as follows. Section 2 introduces the definition and fundamental equations of tensegrity structures. The terminology of the graph theory is used in this exposition, especially for readers who are familiar with operations research but not with applied mechanics. Section 3 presents the constraints and the objective function considered in the topology optimization of tensegrity structures. In Section 4, the optimization problem is reduced to an MILP problem. Three numerical examples are demonstrated in Section 5. We conclude in Section 6.

2. Fundamentals of Tensegrity Structures

As an initial solution for optimization, consider a structure constructed with some straight structural components called *members*. The ends of the members are connected at joints called *nodes*. Each node is a pin joint, which means that members connected to a node can rotate around the node without friction. External forces are considered to be applied only at the nodes. Therefore, an internal force transmitted by a member is only an axial force, which is either tensile or compressive. Such a structure is referred to as a *truss*. The locations of nodes of a truss are specified in the three-dimensional space, when no external force is applied. This configuration is called the initial configuration. Throughout the paper, we assume that deformation of a structure is small and that members consist of a linear elastic material.

Let V and E denote the set of nodes and the set of members of a truss, respectively, where $|V| = n$ and $|E| = m$. For simplicity, we assume $E = \{1, \ldots, m\}$. If we adopt the terminology of the graph theory, V and E correspond to the set of vertices and the set of edges of a graph $G = (V, E)$, respectively. Unlike the graph theory, however, the location is assigned to each node of the truss.

Figure 2 shows an initial configuration of a truss consisting of $|E| = 15$ members connected by $|V| = 6$ nodes. The nodes of this truss form two horizontal equilateral triangles. This paper proposes an optimization-based method for finding a tensegrity structure, regarded as a special truss, from a given initial truss. Figure 1 is a tensegrity structure obtained from the initial structure in Figure 2. Note that three members are removed from Figure 2 to obtain the tensegrity structure in Figure 1.

Let q_i denote the axial force of member i ($i \in E$) introduced in the initial configuration. Here, $q_i > 0$ means that the axial force is tensile, while $q_i < 0$ means that it is compressive. In a tensegrity structure, a member transmitting a compressive force is called a *strut*, while that transmitting a tensile force is called a *cable*. Let $\{S, C, N\}$ be a partition of E defined by

$$S = \{i \in E \mid q_i < 0\}, \tag{2.1a}$$

$$C = \{i \in E \mid q_i > 0\}, \tag{2.1b}$$

$$N = \{i \in E \mid q_i = 0\}, \tag{2.1c}$$

where S, C, and N are the sets of struts, cables, and removed members from the initial structure, respectively. Finding a tensegrity structure from an initial structure is to determine S, C, and N satisfying some particular conditions introduced below; see Definition 2.1. For example, a tensegrity structure in Figure 1 consists of $|S| = 3$ struts and $|C| = 9$ cables, while $|N| = 3$ members are removed from the initial structure in Figure 2. Note that struts are represented by thick lines and cables are represented by thin lines. This is because, in a real-world tensegrity structure, bars with large cross-sections (e.g., stainless-steel tubes) are often used for struts, while cables (e.g., stranded wires) usually have smaller cross-sections than struts.

Let $\boldsymbol{f} \in \mathbb{R}^{3n}$ denote the vector of external forces. The static equilibrium condition, or the force-balance equation, is written as

$$H\boldsymbol{q} = \boldsymbol{f}, \tag{2.2}$$

where $H \in \mathbb{R}^{3n \times m}$ is a constant matrix called the equilibrium matrix. This matrix is obtained as follows. We first determine a direction of each member to obtain a directed

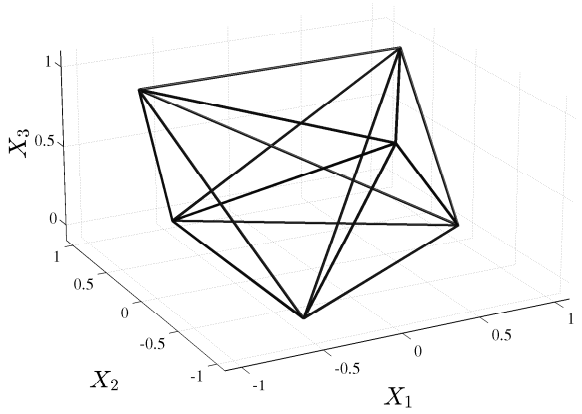

Figure 2: An initial structure to obtain the tensegrity structure in Figure 1

graph $G = (V, E)$, where V and E are regarded as the sets of vertices and edges of G, respectively. Let $D \in \mathbb{R}^{n\times m}$ denote the incidence matrix of G. Define $B_i \in \mathbb{R}^{3\times 3n}$ by $B_i = -\boldsymbol{d}_i^{\mathrm{T}} \otimes I_3$, where $\boldsymbol{d}_i \in \mathbb{R}^n$ is the ith column vector of D, I_3 is the 3×3 identity matrix, and the Kronecker product is designated by $\otimes$. Let $\boldsymbol{x} \in \mathbb{R}^{3n}$ denote the vector consisting of the location vectors of all nodes in the three-dimensional space. Then the ith column vector of H, denoted by $\boldsymbol{h}_i$, is given by $\boldsymbol{h}_i = (1/l_i)B_i^{\mathrm{T}} B_i \boldsymbol{x}$, where l_i is the length of member i. Thus, H is a matrix determined by the connectivity of members and the locations of nodes of the initial structure. Note that (2.2) is similar to the flow conservation condition of the network flow; the vertex v_p at which $f_j \neq 0$ corresponds to a source or a sink and $\boldsymbol{q}$ corresponds to a flow. Unlike the network flow, however, q_i's in (2.2) possibly take negative values and each node has three balance equations corresponding to the coordinates of the three-dimensional space.

We say that the structure is at the state of *self equilibrium* if it sustains $\boldsymbol{q} \neq \boldsymbol{0}$ satisfying (2.2) with $\boldsymbol{f} = \boldsymbol{0}$. It should be clear that self-weight loads are regarded as external loads and hence are not considered at the self-equilibrium state. The axial force q_i at the self-equilibrium state is introduced as a prestress force. Once the self-equilibrium configuration is found, we usually apply the specified external load to the structure to investigate the deformation from the self-equilibrium state.

Let $E(v_p) \subset E$ denote the set of indices of the members that are connected to the node $v_p \in V$. A tensegrity structure is defined in terms of prestress forces $\boldsymbol{q}$ as follows.

Definition 2.1. A truss is said to be a tensegrity structure if there exists $\boldsymbol{q} \neq \boldsymbol{0}$ satisfying

$$H\boldsymbol{q} = \boldsymbol{0}, \tag{2.3}$$

$$|S \cap E(v_p)| \leq 1, \quad \forall v_p \in V, \tag{2.4}$$

where S is defined by (2.1a). ■

Condition (2.3) together with $\boldsymbol{q} \neq \boldsymbol{0}$ requires that a tensegrity structure has a self-equilibrium state. This means that $m - \operatorname{rank} H \geq 1$. Here, $d_{\mathrm{s}} = m - \operatorname{rank} H$ is called the *degree of static indeterminacy*. We say that a structure is statically determinate if $d_{\mathrm{s}} = 0$ and that it is statically indeterminate if $d_{\mathrm{s}} \geq 1$. On the other hand, the *degree of kinematic indeterminacy* is defined by $d_{\mathrm{k}} = 3n - \operatorname{rank} H^{\mathrm{T}} - 6$. The member elongations, denoted $\boldsymbol{c}$, can be written in terms of the nodal displacements, denoted $\boldsymbol{u}$, as $\boldsymbol{c} = H^{\mathrm{T}}\boldsymbol{u}$. Therefore, a nontrivial solution to $H^{\mathrm{T}}\boldsymbol{u} = \boldsymbol{0}$ corresponds to nodal displacements without member elongations. Since the number of degrees of freedom of rigid body motion is six, d_{k} represents

the number of degrees of freedom of infinitesimal deformations that cause no member elongation. In other words, a structure with $d_{\mathrm{k}} > 1$ can deform infinitesimally without applying any external forces. Such a structure is said to be kinematically indeterminate (or unstable). In contrast, if $d_{\mathrm{k}} = 0$, then we say that the structure is kinematically determinate (or stable). Since $\operatorname{rank} H = \operatorname{rank} H^{\mathrm{T}}$, we obtain

$$m - d_{\mathrm{s}} = 3n - d_{\mathrm{k}} - 6, \tag{2.5}$$

which is called the *extended Maxwell rule* [7, 14]. It is known that the tensegrity structure in Figure 1 satisfies $d_{\mathrm{s}} = d_{\mathrm{k}} = 1$, i.e., both statically and kinematically indeterminate, and hence it is unstable. By introducing prestress forces, however, this tensegrity structure can be stabilized [9]. As such this is an "usual" structure and attracts interests of many researchers and artists. A kinematically indeterminate structure stabilized by introducing prestress forces is said to be *prestress stable*. Finding a new tensegrity structure that is prestress stable is an extremely challenging problem. Issues of stability are not taken into account in this paper; particularly, Definition 2.1 does not require prestress stability.

Condition (2.4), called the discontinuity condition of struts, requires that any two struts of a tensegrity structure do not share a common node. In other words, S is a matching of the graph $G = (V, E)$. The discontinuity condition of struts is an intrinsically difficult condition when we attempt to design a new tensegrity structure. Note that Definition 2.1 is one of the most classical definitions of a tensegrity structure; the concept of tensegrity structures has been extended in various ways [24].

3. Compliance Optimization under Self-Weight Load

An optimization problem of tensegrity structures considering the self-weight load is formulated.

3.1. Practical constraints on prestress forces

By definition, the prestress force, q_i, of a tensegrity structure is required to satisfy (2.1). From a practical point of view, however, it is not accepted to apply a very large force to a member. On the other hand, a very small tensile force, which often causes cable sag, should also be avoided from view points of maintainability and visual clarity. Therefore, instead of (2.1), we impose the lower and upper bound constraints for the prestress force as

$$q_i \in \begin{cases} [-\overline{q}^{\mathrm{s}}, -\underline{q}^{\mathrm{s}}] & \text{if } i \in S, \\ [\underline{q}^{\mathrm{c}}, \overline{q}^{\mathrm{c}}] & \text{if } i \in C, \\ \{0\} & \text{if } i \in N, \end{cases} \tag{3.1}$$

where $\underline{q}^{\mathrm{s}}$, $\overline{q}^{\mathrm{s}}$, $\underline{q}^{\mathrm{c}}$, and $\overline{q}^{\mathrm{c}}$ are positive constants satisfying $\underline{q}^{\mathrm{s}} < \overline{q}^{\mathrm{s}}$ and $\underline{q}^{\mathrm{c}} < \overline{q}^{\mathrm{c}}$.

Besides (3.1), $\boldsymbol{q}$ should satisfy the self-equilibrium condition introduced in (2.3).

3.2. Member cross-sectional areas

It is often that a real-world tensegrity structure is constructed by using thick bars for struts and thin wires for cables. We denote by ξ^{s} and ξ^{c} ($\xi^{\mathrm{s}} > \xi^{\mathrm{c}}$) the specified cross-sectional areas of such bars and wires, respectively. Then the cross-sectional area of member i, denoted a_i, is given by

$$a_i = \begin{cases} \xi^{\mathrm{s}} & \text{if } i \in S, \\ \xi^{\mathrm{c}} & \text{if } i \in C, \\ 0 & \text{if } i \in N. \end{cases} \tag{3.2}$$

The elongation stiffness of member i, which represents the axial force caused by a unit elongation, is written as

$$k_i = \frac{Ya_i}{l_i}, \tag{3.3}$$

where Y is the Young modulus. Precisely, the elongation stiffness should be defined by using the initial (i.e., undeformed) member length, l_i^0, as Ya_i/l_i^0. Due to the presence of prestress forces, the member length of the initial structure, l_i, is not equal to l_i^0. However, the difference between l_i and l_i^0 is negligibly small. Hence, in this paper we define the member elongation stiffness by (3.3).

3.3. Equilibrium state under self-weight load

Usually a tensegrity structure transfers the applied external load (including its self-weight load) to the ground (or a foundation). The connections which join a structure to its foundation are called *supports*. In Section 3.1 we have assumed that the tensegrity structure does not have supports to study the self-equilibrium state at which no external load is applied. In contrast, we here suppose that some of degrees of freedom of the displacements are fixed by supports to investigate its equilibrium state in the presence of the external load.

Let $\boldsymbol{u} \in \mathbb{R}^{3n}$ denote the vector of nodal displacements. Consider a partition $J_{\rm D} \cup J_{\rm N} = \{1, \ldots, 3n\}$ of the set of indices of the degrees of freedom of displacements. Suppose that the displacement for each $j \in J_{\rm D}$ is fixed by a support as $u_j = 0$ and that the external force for each $j \in J_{\rm N}$ is specified as f_j. Since the self-weight load is a function of the member cross-sectional areas, $\boldsymbol{a}$, we write $f_j(\boldsymbol{a})$ in what follows. We use s_i to denote the axial force equilibrated with the external load. The force balance between s_i $(i = 1, \ldots, m)$ and $f_j(\boldsymbol{a})$ $(j \in J_{\rm N})$ can be written by using the equilibrium matrix H introduced in (2.2). Summing up the support conditions and the force-balance conditions, $\boldsymbol{u}$ and $\boldsymbol{s}$ should satisfy

$$u_j = 0, \qquad \forall j \in J_{\rm D}, \tag{3.4}$$

$$(H\boldsymbol{s})_j = f_j(\boldsymbol{a}), \quad \forall j \in J_{\rm N}, \tag{3.5}$$

where $(H\boldsymbol{s})_j$ is the jth component of the vector $H\boldsymbol{s}$. Note that the prestress force q_i presents before applying the external load. In other words, the total axial force at the equilibrium state, denoted $\tilde{s}_i$, is given by

$$\tilde{s}_i = q_i + s_i. \tag{3.6}$$

The equilibrium state is characterized by three conditions: the force-balance equation (i.e., (3.5)), the compatibility relation, and the constitutive law. Let c_i denote the elongation of member i. The compatibility relation that associates c_i with $\boldsymbol{u}$ can be written by using the column vector of H as

$$c_i = \boldsymbol{h}_i^{\rm T}\boldsymbol{u}, \quad i = 1, \ldots, m. \tag{3.7}$$

The constitutive law gives the relation between c_i and s_i. By using the elongation stiffness defined by (3.3), it can be written as

$$s_i = k_i c_i, \quad i = 1, \ldots, m. \tag{3.8}$$

The upshot is that, for the given external load $f_j(\boldsymbol{a})$ $(j \in J_{\rm N})$, the equilibrium state is found as the solution of (3.4), (3.5), (3.7), and (3.8).

We also consider the upper and lower bound constraints for the axial forces at the equilibrium state under the self-weight load. Specifically, the total axial force, i.e., $\tilde{s}_i$ in (3.6), should satisfy

$$q_i + s_i \in \begin{cases} [-\overline{s}^{\mathrm{s}}, -\underline{s}^{\mathrm{s}}] & \text{if } i \in S, \\ [\underline{s}^{\mathrm{c}}, \overline{s}^{\mathrm{c}}] & \text{if } i \in C. \end{cases} \tag{3.9}$$

Here, $\underline{s}^{\mathrm{s}}$, $\overline{s}^{\mathrm{s}}$, $\underline{s}^{\mathrm{c}}$, and $\overline{s}^{\mathrm{c}}$ are positive constants satisfying $\underline{s}^{\mathrm{s}} < \overline{s}^{\mathrm{s}}$ and $\underline{s}^{\mathrm{c}} < \overline{s}^{\mathrm{c}}$. Note that for $i \in N$ no constraint is considered on the axial force.

3.4. Constraints on existing members

By definition, the struts should satisfy the discontinuity condition introduced in (2.4). Besides this condition, we consider other constraints on number of members to restrict the feasible solutions to attractive tensegrity structures.

To find complex tensegrity structures, it is natural to attempt to use many struts. This motivates us to consider the constraint

$$|S| \geq n^{\mathrm{s}}, \tag{3.10}$$

where n^{s} is the specified lower bound for the number of struts.

Roughly speaking, a tensegrity structure with less cables is more interesting when the number of struts is fixed. Some of existing tensegrity structures, especially that are created as arts, are prestress stable. Recall that stability is related to d_{k}, the degree of kinematic indeterminacy: $d_{\mathrm{k}} = 0$ if the tensegrity structure is stable, while $d_{\mathrm{k}} > 0$ if it is unstable. On the other hand, a tensegrity structure satisfies $d_{\mathrm{s}} \geq 1$, because it satisfies (2.3) by definition. Therefore, every stable tensegrity structure satisfies $d_{\mathrm{k}} - d_{\mathrm{s}} \leq -1$. An unstable tensegrity structure illustrated in Figure 1 satisfies $d_{\mathrm{k}} - d_{\mathrm{s}} = 0$. Hence, we attempt to explore tensegrity structures with large values of $d_{\mathrm{k}} - d_{\mathrm{s}}$, e.g., $d_{\mathrm{k}} - d_{\mathrm{s}} = -1, 0, 1$. Since many tensegrity structures do not have a node that are connected to cables only, we substitute

$$m = |S| + |C|, \quad n = 2|S|$$

into (2.5) to obtain $d_{\mathrm{k}} - d_{\mathrm{s}} = 5|S| - |C| - 6$. Accordingly, we consider the constraint

$$5|S| - |C| - 6 = n^{\mathrm{d}} \tag{3.11}$$

where n^{d} is the specified value of $d_{\mathrm{k}} - d_{\mathrm{s}}$. In other words, the larger the value of n^{d}, the less the number of cables when the number of struts is fixed.

A more practical constraint was introduced in [21]. It is often that an initial structure includes many intersecting members; see, e.g., Figure 3 in Section 5.1. In a tensegrity structure obtained from the initial structure, presence of mutually intersecting members is not accepted. Practically, two members that are too close cannot exist simultaneously. The set of such pairs of members is denoted by P_{cross}. Precisely, we write $(i, i') \in P_{\mathrm{cross}}$ if the distance of member i and member i' is less than a specified threshold δ ($\delta > 0$). Then the constraint excluding too close members is formally written as

$$\{i, i'\} \not\subseteq S \cup C, \quad \forall (i, i') \in P_{\mathrm{cross}}. \tag{3.12}$$

3.5. Optimization problem of tensegrity structures

Since tensegrity structures are relatively flexible in general, the self-weight load may possibly affect a tensegrity structure significantly compared with other stiff structures such as trusses and frames. For example, if only prestress forces are taken into consideration in the design process, then the configuration of the actually constructed tensegrity structure under the force of gravity may become much different from the expected one. Moreover, due to such difference of configurations, some cables may become slack and/or tensile forces may be introduced to some struts unanticipatedly. Thus it is inevitable to consider the self-weight load in designing a tensegrity structure. This is actually the motivation of the present work.

To prevent unanticipated deformation due to the self-weight, it might be natural to explore a structure which is stiff against the self-weight load. Finding a stiff structure is usually performed by minimizing the *compliance*, which is the work done by the applied external load. If the Dirichlet boundary conditions are homogeneous (that is the case with our problem as seen in (3.4)), then the compliance is equal to the elastic energy stored in the structure. Therefore, the compliance can be regarded as a measure of flexibility of a structure. Let $\boldsymbol{u}$ be the displacement vector at the equilibrium state, i.e., be a solution of (3.4), (3.5), (3.7) and (3.8). Then the compliance, denoted w, is defined by

$$w = \sum_{j \in J_{\mathrm{N}}} f_j(\boldsymbol{a}) u_j. \tag{3.13}$$

Note that in this paper we define the compliance as the external work done only by the self-weight load. In other words, the internal work due to the prestress forces $\boldsymbol{q}$ is not considered in (3.13).

We are now in position to formulate an optimization problem for designing a tensegrity structure. The constraints of the problem consist of the following four conditions: (i) the prestress forces should satisfy (2.3) and (3.1); (ii) the equilibrium condition under the self-weight load is described by (3.4), (3.5), (3.7), and (3.8), where the member cross-sectional areas and the elongation stiffness are defined by (3.2) and (3.3); (iii) at that equilibrium state the axial forces should satisfy (3.9); (iv) regarding existing members we consider the constraints (2.4), (3.10), (3.11), and (3.12). Under these constraints, we find the structure that minimizes the compliance defined by (3.13).

Thus the optimization problem of tensegrity structures is a nonconvex optimization problem. Particularly, the constraints depend on the partition $\{S, C, N\}$ of E. Therefore, nonlinear programming approaches are likely to be inefficient. This motivates us to reformulate the optimization problem as an MILP problem, which is the subject of the next section.

4. Mixed Integer Linear Programming Formulation

The optimization problem presented in Section 3 is reduced to an MILP problem.

4.1. Constraints on member forces

A difficulty of optimization of structures considering the self-weight load stems from the fact that the self-weight load depends on the design variables. In contrast, an optimization problem of tensegrity structures subjected to a fixed external load was reduced to an MILP problem in [21]. We briefly recall, here, the formulations in [21] concerning the labels of members and the stress constraints under a fixed external load. The constraints involving the self-weight load will be addressed in Section 4.3.

An essential idea presented in [21] is introducing two 0–1 variables, x_i and y_i, to represent the classification of member i as

$$(x_i, y_i) = (1, 0) \quad \Leftrightarrow \quad i \in S, \tag{4.1a}$$
$$(x_i, y_i) = (0, 1) \quad \Leftrightarrow \quad i \in C, \tag{4.1b}$$
$$(x_i, y_i) = (0, 0) \quad \Leftrightarrow \quad i \in N. \tag{4.1c}$$

The case $(x_i, y_i) = (1, 1)$ is excluded, i.e.,

$$x_i + y_i \leq 1. \tag{4.2}$$

Moreover, we rewrite the compatibility relation, (3.7), as

$$c_i^{\mathrm{s}} = \begin{cases} \boldsymbol{h}_i^{\mathrm{T}} \boldsymbol{u} & \text{if } i \in S, \\ 0 & \text{otherwise}, \end{cases} \tag{4.3}$$

$$c_i^{\mathrm{c}} = \begin{cases} \boldsymbol{h}_i^{\mathrm{T}} \boldsymbol{u} & \text{if } i \in C, \\ 0 & \text{otherwise}. \end{cases} \tag{4.4}$$

That is, c_i^{s} represents the elongation of a strut and c_i^{c} represents that of a cable. The constitutive law, (3.8), is then reduced to

$$s_i = k_i^{\mathrm{s}} c_i^{\mathrm{s}} + k_i^{\mathrm{c}} c_i^{\mathrm{c}}, \tag{4.5}$$

where

$$k_i^{\mathrm{s}} = \frac{E\xi^{\mathrm{s}}}{l_i}, \quad k_i^{\mathrm{c}} = \frac{E\xi^{\mathrm{c}}}{l_i}.$$

Thus, (3.2), (3.3), (3.7), and (3.8) are equivalently rewritten as (4.3), (4.4), and (4.5). Note that (4.3), (4.4), and (4.5) imply $s_i = 0$ for $i \in N$ as expected.

The upper and lower bound constraints on axial forces are introduced in (3.1) and (3.9). We rewrite these constraints in terms of q_i, c_i^{s}, and c_i^{c} together with the member label (x_i, y_i). Suppose that (4.1) and (4.3), (4.4), (4.5) are satisfied. Then we can see that q_i and s_i satisfy (3.1) and (3.9) if and only if the linear inequalities

$$\underline{q}^{\mathrm{c}} y_i - \overline{q}^{\mathrm{s}}(1 - y_i) \leq q_i \leq -\underline{q}^{\mathrm{s}} x_i + \overline{q}^{\mathrm{c}}(1 - x_i), \tag{4.6a}$$
$$-\overline{s}^{\mathrm{s}} x_i \leq q_i + k_i^{\mathrm{s}} c_i^{\mathrm{s}} \leq -\underline{s}^{\mathrm{s}} x_i + \overline{q}^{\mathrm{c}} y_i, \tag{4.6b}$$
$$-\overline{q}^{\mathrm{s}} x_i + \underline{s}^{\mathrm{c}} y_i \leq q_i + k_i^{\mathrm{c}} c_i^{\mathrm{c}} \leq \overline{s}^{\mathrm{c}} y_i \tag{4.6c}$$

are satisfied.

Remark 4.1. If $(x_i, y_i) = (1, 1)$, then (4.6a) is reduced to $\underline{q}^{\mathrm{c}} \leq q_i \leq -\underline{q}^{\mathrm{s}}$. Therefore, (4.6a) implies (4.2). In the MILP problem presented in Section 4.4, we use (4.2) as a valid inequality constraint. ■

Finally we rewrite (4.3) and (4.4) as linear inequalities with binary variables. We again use x_i and y_i defined by (4.1). For $i \in S$, it follows from (4.6a) and (4.6b) that q_i and c_i^{s} are subjected to the following constraints:

$$-\overline{q}^{\mathrm{s}} \leq q_i \leq -\underline{q}^{\mathrm{s}},$$
$$-\overline{s}^{\mathrm{s}} \leq q_i + k_i^{\mathrm{s}} c_i^{\mathrm{s}} \leq -\underline{s}^{\mathrm{s}}.$$

These inequalities imply

$$\underline{q}^{\mathrm{s}} - \overline{s}^{\mathrm{s}} \leq k_i^{\mathrm{s}} c_i^{\mathrm{s}} \leq \overline{q}^{\mathrm{s}} - \underline{s}^{\mathrm{s}}.$$

Therefore, (4.3) can be rewritten as

$$(\underline{q}^{\mathrm{s}} - \overline{s}^{\mathrm{s}}) x_i \leq k_i^{\mathrm{s}} c_i^{\mathrm{s}} \leq (\overline{q}^{\mathrm{s}} - \underline{s}^{\mathrm{s}}) x_i, \tag{4.8a}$$

$$M(1 - x_i) \geq |c_i^{\mathrm{s}} - \boldsymbol{h}_i^{\mathrm{T}} \boldsymbol{u}|, \tag{4.8b}$$

where $M \gg 0$ is a sufficiently large constant. Similarly, (4.4) can be rewritten as

$$(\underline{s}^{\mathrm{c}} - \overline{q}^{\mathrm{c}}) y_i \leq k_i^{\mathrm{c}} c_i^{\mathrm{c}} \leq (\overline{s}^{\mathrm{c}} - \underline{q}^{\mathrm{c}}) y_i, \tag{4.9a}$$

$$M(1 - y_i) \geq |c_i^{\mathrm{c}} - \boldsymbol{h}_i^{\mathrm{T}} \boldsymbol{u}|. \tag{4.9b}$$

4.2. Constraints on member labels

In Section 4.1 we have introduced variables $(x_i, y_i) \in \{0, 1\}^2$ by (4.1) to formulate the constraints concerning the equilibrium state under the specified external load. As the other constraints in terms of x_i and y_i, we here investigate the constraints on the numbers of struts and cables.

We first consider the discontinuity condition of struts, (2.4). This constraint can be written in terms of x_i $(i \in E)$ as

$$\sum_{i \in E(v_p)} x_i \leq 1, \quad \forall v_p \in V. \tag{4.10}$$

The lower bound constraint on the total number of struts was given by (3.10), which is reduced to

$$\sum_{i \in E} x_i \geq n^{\mathrm{s}}. \tag{4.11}$$

The relation between the number of struts and that of cables was given by (3.11). This constraint can be written as

$$\sum_{i \in E} (5x_i - y_i) = n^{\mathrm{d}} + 6. \tag{4.12}$$

Constraint (3.12) was introduced to prevent two close members from existing together. This constraint can be written in terms of x_i and y_i as

$$x_i + x_{i'} + y_i + y_{i'} \leq 1, \quad \forall (i, i') \in P_{\mathrm{cross}}. \tag{4.13}$$

4.3. Compliance under self-weight load

We here discuss the compliance constraint under the self-weight load in the framework of MILP. In the force-balance equation, (3.5), the self-weight load is denoted by $\boldsymbol{f}(\boldsymbol{a})$. For simplicity, the gravity forces acting on cables are neglected, because in many real-life tensegrity structures struts are much heavier than cables. Hence, $\boldsymbol{f}(\boldsymbol{a})$ is the sum of gravity forces acting on struts. Since the member cross-sectional area, a_i, is given by (3.2), $\boldsymbol{f}(\boldsymbol{a})$ can be written as

$$\boldsymbol{f}(\boldsymbol{a}) = \sum_{i \in E} x_i \xi^{\mathrm{s}} \boldsymbol{f}^{(i)}, \tag{4.14}$$

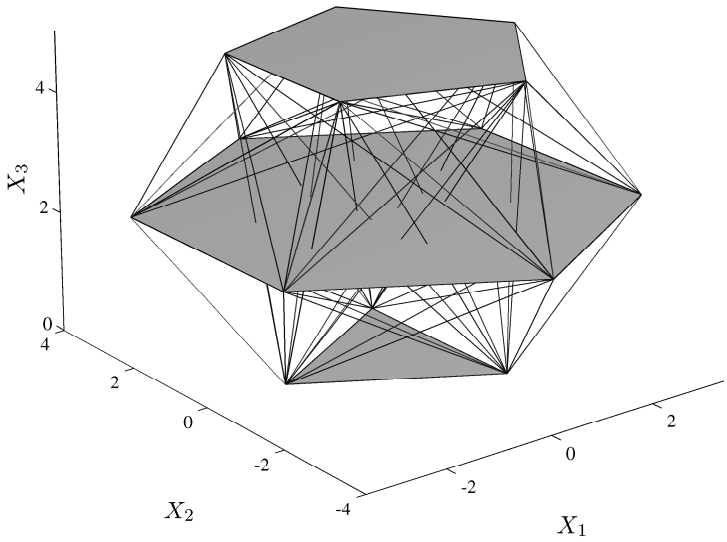

Figure 3: An initial structure with three layers

where $\boldsymbol{f}^{(i)}$ is the gravity force vector of a unit cross-sectional area of member i.

The compliance, w, is then given by (3.13) with $f_j(\boldsymbol{a})$ in (4.14). Define extra variables w_i $(i \in E)$ by

$$w_i = \begin{cases} \displaystyle\sum_{j \in J_{\mathrm{N}}} f_j^{(i)} u_j & \text{if } i \in S, \\ 0 & \text{otherwise.} \end{cases} \tag{4.15}$$

Then (3.13) is rewritten as

$$w = \sum_{i \in E} w_i. \tag{4.16}$$

On the other hand, by using x_i, (4.15) is rewritten as

$$M x_i \geq |w_i|, \tag{4.17a}$$

$$M(1 - x_i) \geq \left| w_i - \sum_{j \in J_{\mathrm{N}}} f_j^{(i)} u_j \right|, \tag{4.17b}$$

where M is a sufficiently large constant. Thus, minimizing the compliance of a tensegrity structure is realized by minimizing w in (4.16) under constraint (4.17).

4.4. MILP formulation

We are now in position to formulate an MILP problem for topology optimization of tensegrity structures. The optimization problem was defined in Section 3.5. To reformulate this problem, the constraints on member forces were reduced to linear inequalities in Section 4.1 by introducing 0–1 variables, x_i and y_i. Section 4.2 dealt with the constraints regarding the numbers of struts and cables. In Section 4.3, the compliance constraint under the self-weight load was expressed by using linear inequalities including x_i.

The upshot is that the optimization problem of tensegrity structures can be written as

$$
\left.
\begin{array}{lll}
\min\limits_{\boldsymbol{x},\boldsymbol{y},\boldsymbol{q},\boldsymbol{s},\boldsymbol{c}^{\mathrm{s}},\boldsymbol{c}^{\mathrm{c}},\boldsymbol{u},\boldsymbol{w}} & \displaystyle\sum_{i\in E} w_i & \\
\text{s.t.} & H\boldsymbol{q}=\boldsymbol{0}, & \\
& \underline{q}^{\mathrm{c}} y_i - \overline{q}^{\mathrm{s}}(1-y_i) \le q_i \le -\underline{q}^{\mathrm{s}} x_i + \overline{q}^{\mathrm{c}}(1-x_i), & \forall i, \\
& (H\boldsymbol{s})_j = \displaystyle\sum_{i\in E} x_i \xi^{\mathrm{s}} f_j^{(i)}, & \forall j\in J_{\mathrm{N}}, \\
& u_j = 0, & \forall j\in J_{\mathrm{D}}, \\
& s_i = k_i^{\mathrm{s}} c_i^{\mathrm{s}} + k_i^{\mathrm{c}} c_i^{\mathrm{c}}, & \forall i, \\
& -(\overline{s}^{\mathrm{s}} - \underline{q}^{\mathrm{s}}) x_i \le k_i^{\mathrm{s}} c_i^{\mathrm{s}} \le -(\underline{s}^{\mathrm{s}} - \overline{q}^{\mathrm{s}}) x_i, & \forall i, \\
& (\underline{s}^{\mathrm{c}} - \overline{q}^{\mathrm{c}}) y_i \le k_i^{\mathrm{c}} c_i^{\mathrm{c}} \le (\overline{s}^{\mathrm{c}} - \underline{q}^{\mathrm{c}}) y_i, & \forall i, \\
& M(1-x_i) \ge |c_i^{\mathrm{s}} - \boldsymbol{h}_i^{\mathrm{T}}\boldsymbol{u}|, & \forall i, \\
& M(1-y_i) \ge |c_i^{\mathrm{c}} - \boldsymbol{h}_i^{\mathrm{T}}\boldsymbol{u}|, & \forall i, \\
& -\overline{s}^{\mathrm{s}} x_i \le q_i + k_i^{\mathrm{s}} c_i^{\mathrm{s}} \le -\underline{s}^{\mathrm{s}} x_i + \overline{q}^{\mathrm{c}} y_i, & \forall i, \\
& -\overline{q}^{\mathrm{s}} x_i + \underline{s}^{\mathrm{c}} y_i \le q_i + k_i^{\mathrm{c}} c_i^{\mathrm{c}} \le \overline{s}^{\mathrm{c}} y_i, & \forall i, \\
& Mx_i \ge |w_i|, \quad M(1-x_i) \ge \left| w_i - \displaystyle\sum_{j\in J_{\mathrm{N}}} f_j^{(i)} u_j \right|, & \forall i, \\
& \displaystyle\sum_{i\in E(v_p)} x_i \le 1, & \forall v_p \in V, \\
& \displaystyle\sum_{i\in E} x_i \ge n^{\mathrm{s}}, \quad 5\sum_{i\in E} x_i - \sum_{i\in E} y_i - 6 = n^{\mathrm{d}}, & \\
& x_i + x_{i'} + y_i + y_{i'} \le 1, & \forall (i,i') \in P_{\mathrm{cross}}, \\
& x_i \in \{0,1\}, \quad y_i \in \{0,1\}, \quad x_i + y_i \le 1, & \forall i.
\end{array}
\right\} \tag{4.18}
$$

This is an MILP problem. In Section 5 we solve this MILP problem by using commercial solvers, CPLEX [17] and Gurobi Optimizer [15]. Note that this problem includes a large constant M. It is well known that such a "big-M" should not be chosen larger than necessary, because constraints including unnecessarily large M often slow down the solution process. Unfortunately, it is not easy to guess the smallest value of M for this problem in advance.

5. Numerical Experiments

The optimal topologies of various tensegrity structures are found by solving problem (4.18). Computation was carried out on two 2.66 GHz 6-Core Intel Xeon Westmere processors with 64 GB RAM. The data of MILP problem (4.18) were prepared with MATLAB Ver. 7.9 in the CPLEX LP file format. Then, for comparison, the MILP problem was solved by using CPLEX Ver. 12.2 [17] and Gurobi Optimizer Ver. 4.5 [15] with the default options.

In the examples of this section, the material of struts and cables is aluminium, where the Young modulus is $Y = 70\,\mathrm{GPa}$ and the mass density is $\rho = 3\times 10^3\,\mathrm{kg/m^3}$. The member cross-sectional areas of struts and cables are $\xi_{\mathrm{s}} = 2000\,\mathrm{mm^2}$ and $\xi_{\mathrm{c}} = 100\,\mathrm{mm^2}$, respectively. The bounds for prestress forces in (3.1) are $\underline{q}^{\mathrm{s}} = 3.5\,\mathrm{kN}$, $\overline{q}^{\mathrm{s}} = 140\,\mathrm{kN}$, $\underline{q}^{\mathrm{c}} = 1.75\,\mathrm{kN}$, and $\overline{q}^{\mathrm{c}} = 35\,\mathrm{kN}$. For the axial forces under the self-weight load, the bounds in (3.9) are $\underline{s}^{\mathrm{s}} = 7\,\mathrm{kN}$, $\overline{s}^{\mathrm{s}} = 70\,\mathrm{kN}$, $\underline{s}^{\mathrm{c}} = 3.5\mathrm{kN}$, and $\overline{s}^{\mathrm{c}} = 17.5\,\mathrm{kN}$.

5.1. Three-layer tensegrity structure

Consider an initial structure illustrated in Figure 3, where X_1 and X_2 are taken to be two horizontal axes and the vertical axis is denoted by X_3. The structure consists of $|V| = 14$ nodes and $|E| = 77$ members.

Table 1: Computational results of the three layer example

						CPU (s)	
n^{d}	w (J)	$\lvert C\rvert$	$\lvert S\rvert$ $(= n^{\mathrm{s}})$	d_{s}	d_{k}	CPLEX	Gurobi
-1	3.68500	30	7	1	0	512.3	1,078.1
-2	2.75344	31	7	2	0	442.0	650.5
-3	2.35530	32	7	3	0	588.1	465.6

The locations of the nodes of this initial structure are defined as follows. The nodes form three horizontal layers as depicted by shaded polygons in Figure 3, where the centers of these polygons are on the X_3-axis. The bottom layer is in an equilateral triangular shape, the middle one is a regular hexagon, and the top one is a regular pentagon. The lengths of edges of these polygons are $2\sqrt{3}\,\mathrm{m}$, $4\,\mathrm{m}$, and $5\sin\frac{\pi}{5}\,\mathrm{m}$, respectively. Each polygon has an edge which is parallel to the X_2-axis. The distance between the adjacent layers is $2.5\,\mathrm{m}$.

Any two nodes are connected by a member, but members corresponding to the diagonals of hexagonal and pentagonal layers are removed. As stated in Section 3.4, we do not allow two close members to exist simultaneously. The lower bound for the distance of two existing members is $\delta = 0.05\,\mathrm{m}$, which results in $|P_{\mathrm{cross}}| = 17$ pairs of intersecting members for this initial structure. To consider the equilibrium state under the self-weight load, six degrees of freedom of displacements of the bottom nodes are fixed, i.e., $|J_{\mathrm{D}}| = 6$. Specifically, we fix the displacements in all directions of the node at $(1, \sqrt{3}, 0)$, the displacements in the X_1- and X_3-directions of the node at $(1, -\sqrt{3}, 0)$, and the displacement in the X_3-direction of the node at $(-2, 0, 0)$. Then MILP problem (4.18) has $2|E| = 154$ binary variables, $5|E| + 3|V| = 427$ continuous variables, 1495 linear inequality constraints, and 162 linear quality constraints.

As for n^{d} introduced in (3.11), we consider three cases: $n^{\mathrm{d}} = -1$, -2, and -3. The lower bound for the number of struts is $n^{\mathrm{s}} = 7$. The optimal tensegrity structures obtained by solving problem (4.18) are shown in Figure 4, where the thick lines and the thin lines represent struts and cables, respectively. The computational results are listed in Table 1. Here, w means the compliance of the optimal solution, "CPU" is the computational time spent by an MILP solver, $|C|$ is the number of cables, $|S|$ is the number of struts, and d_{s} and d_{k} denote the degrees of static indeterminacy and kinematic indeterminacy, respectively. All the obtained structures are kinematically determinate (i.e., stable). It is observed in Table 1 that as the number of cables increases, the degree of static indeterminacy increases and the compliance decreases. Thus the stiffness against the self-weight load is improved by increasing the number of cables.

In the case of $n^{\mathrm{d}} = -1$, different optimal solutions are found by CPLEX and Gurobi Optimizer; Figures 4(a) and (b) illustrate the solutions obtained by CPLEX and Gurobi Optimizer, respectively. The objective value of the solution by CPLEX is $w = 3.6850015$, while that by Gurobi Optimizer is $w = 3.6850044$. Therefore, the solution provided by Gurobi Optimizer is not a global optimal solution, although the difference of these objective values is subtle.

The optimal solutions shown in Figures 4(a), (c), and (d) share the same set of struts. However, the locations of cables are different. More precisely, for example, the set of cables in Figure 4(a) is not a subset of that in Figure 4(c).

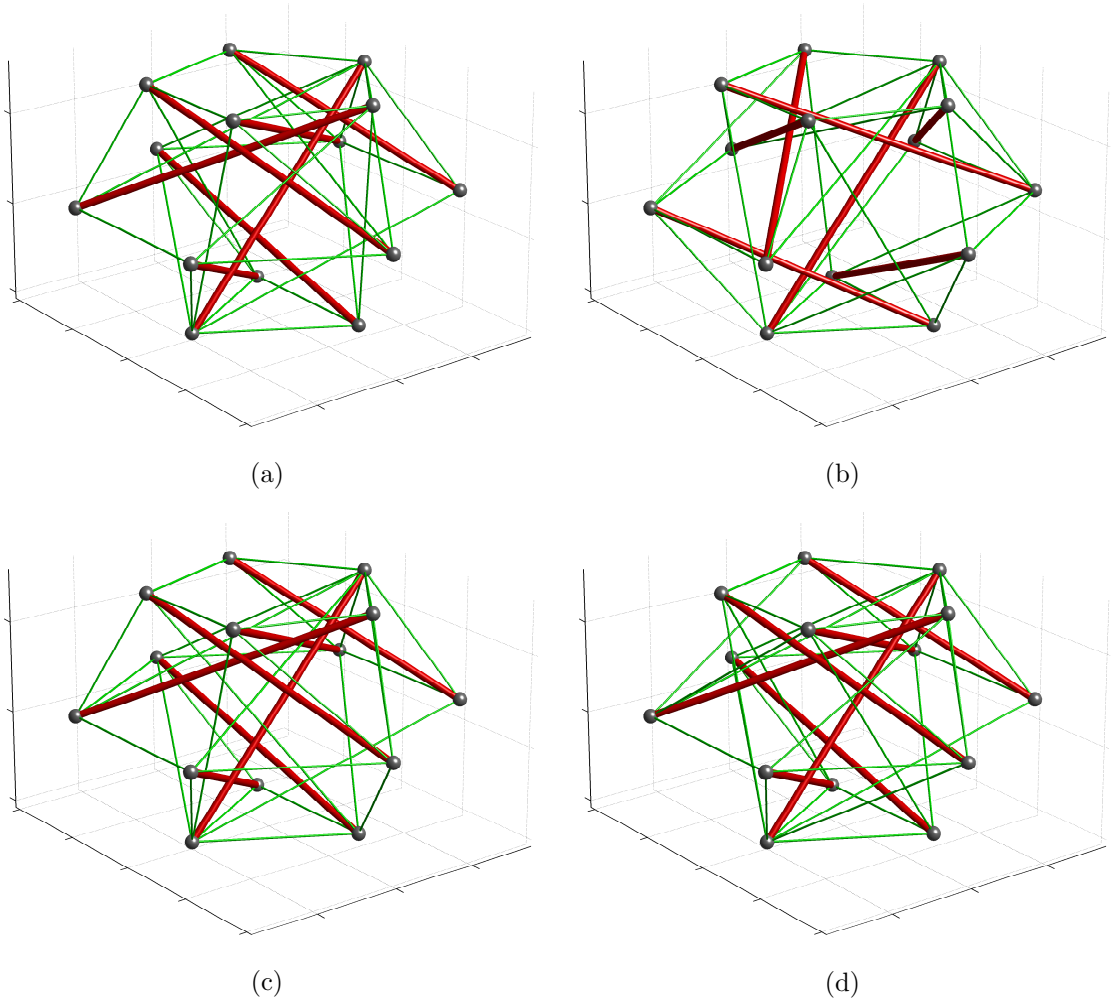

Figure 4: Optimal solutions obtained from the three-layer initial structure in Figure 3. (a) $n^{\mathrm{d}} = -1$ by CPLEX; (b) $n^{\mathrm{d}} = -1$ by Gurobi Optimizer; (c) $n^{\mathrm{d}} = -2$; (d) $n^{\mathrm{d}} = -3$

5.2. Cantilevered tensegrity structure

We next consider an initial structure illustrated in Figure 5. The structure consists of $|V| = 14$ nodes and $|E| = 82$ members. The number of pairs of intersecting members (with threshold $\delta = 0.05\,\mathrm{m}$) is $|P_{\mathrm{cross}}| = 23$.

The locations of the nodes of this initial structure are defined as follows. The nodes form four vertical layers, which are two equilateral triangles and two squares as shown in Figure 5. We call these layers L_1, L_2, L_3, and L_4, where the leftmost one is L_1 and the rightmost one is L_4. The lengths of edges of L_1 and L_4 are $\sqrt{3}\,\mathrm{m}$, while those of L_2 and L_3 are $1.25\sqrt{2}\,\mathrm{m}$. All the layers are parallel to the X_2X_3-plane and their centers are on the X_1-axis. Moreover, each of L_1, L_3, and L_4 has an edge which is parallel to the X_2-axis. Then L_2 is rotated from L_3 counter-clockwise around the X_1-axis with the angle $\pi/12$. The X_1-coordinates of the nodes of L_1, L_2, L_3, and L_4 are $0\,\mathrm{m}$, $4.25\,\mathrm{m}$, $4.75\,\mathrm{m}$, and $9\,\mathrm{m}$, respectively.

Any two nodes of the initial structure are connected by a member, but members connecting the pair L_1 and L_4 are removed to avoid presence of too long members. To consider the equilibrium state under the self-weight load, all the nodes of L_1 are fixed. Therefore, $|J_{\mathrm{D}}| = 9$ and $|J_{\mathrm{N}}| = 33$. Such a structure anchored at only one end on a wall is called a *cantilever*. MILP problem (4.18) includes $2|E| = 164$ binary variables, $5|E| + 3|V| = 452$

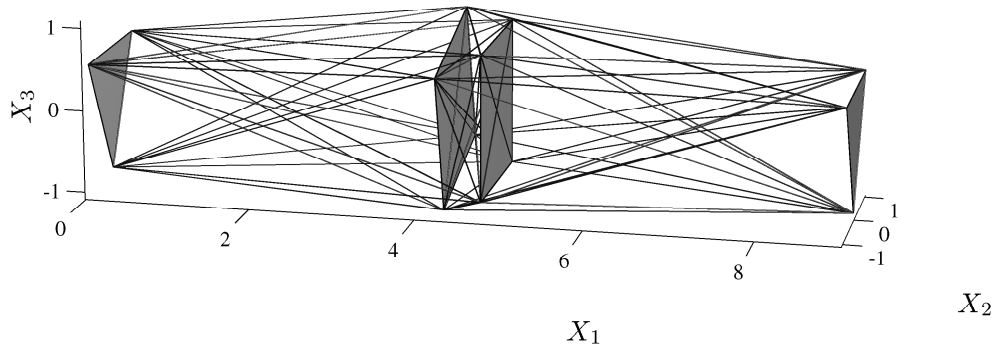

Figure 5: A cantilevered initial structure

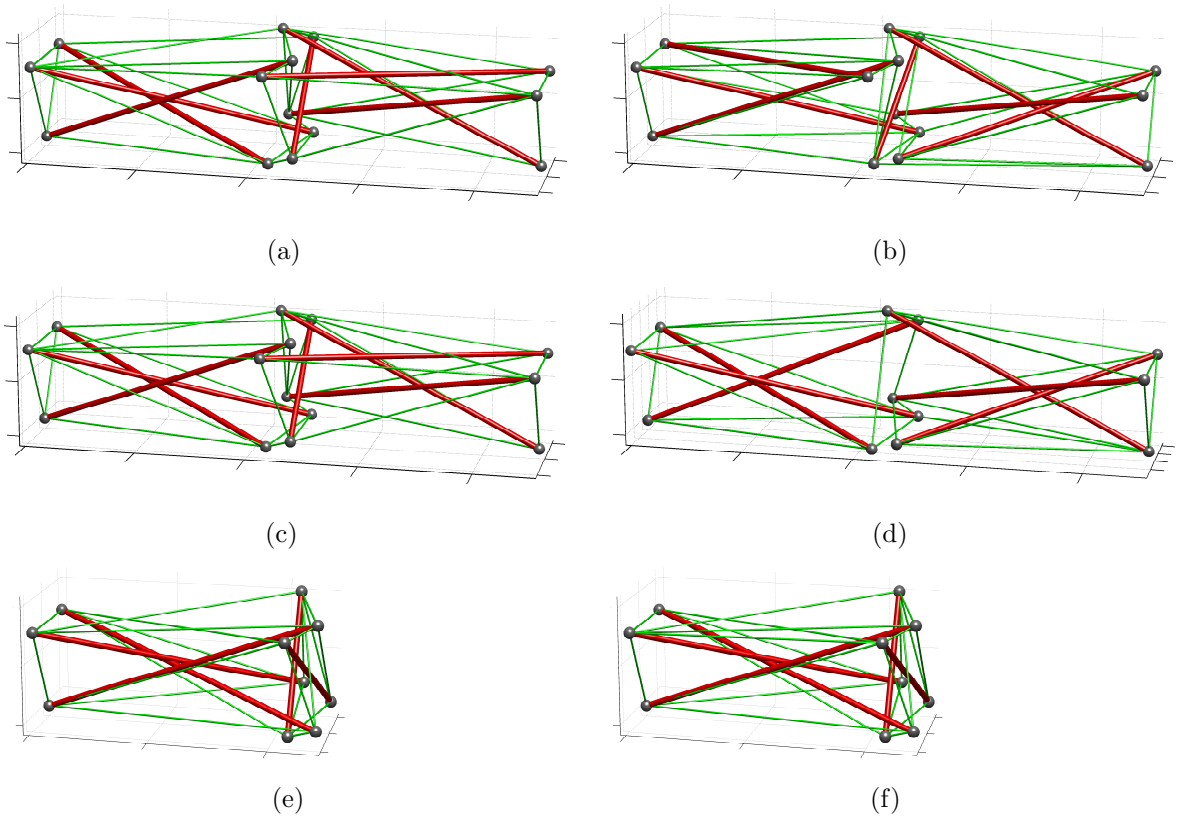

Figure 6: Optimal solutions obtained from the cantilevered initial structure in Figure 5. (a) $(n^{\mathrm{s}}, n^{\mathrm{d}}) = (7, -1)$; (b) $(n^{\mathrm{s}}, n^{\mathrm{d}}) = (7, -2)$; (c) $(n^{\mathrm{s}}, n^{\mathrm{d}}) = (6, -1)$; (d) $(n^{\mathrm{s}}, n^{\mathrm{d}}) = (6, -2)$; (e) $(n^{\mathrm{s}}, n^{\mathrm{d}}) = (5, -1)$; (f) $(n^{\mathrm{s}}, n^{\mathrm{d}}) = (5, -2)$

continuous variables, 1596 linear inequality constraints, and 167 linear equality constraints.

As for n^{s} and n^{d}, we consider nine cases: $n^{\mathrm{s}} = 5, 6, 7$ and $n^{\mathrm{d}} = 0, -1, -2$. The solutions obtained by CPLEX are illustrated in Figure 6. The computational results are listed in Table 2. In each case, the computational time required by Gurobi Optimizer is larger than that required by CPLEX. The three cases with $n^{\mathrm{d}} = 0$ are infeasible problems. The solution obtained for $(n^{\mathrm{s}}, n^{\mathrm{d}}) = (6, -1)$ is same as that for $(n^{\mathrm{s}}, n^{\mathrm{d}}) = (7, -1)$.

In Table 2, the symbol "$*$" means that the solution obtained by Gurobi Optimizer is not a global optimal solution. Indeed, both for $(n^{\mathrm{s}}, n^{\mathrm{d}}) = (6, -2)$ and $(n^{\mathrm{s}}, n^{\mathrm{d}}) = (5, -2)$, Gurobi Optimizer declared the solution for $(n^{\mathrm{s}}, n^{\mathrm{d}}) = (7, -2)$ shown in Figure 6(b) as the optimal

Table 2: Computational results of the cantilevered example

							CPU (s)	
n^{s}	n^{d}	$w\,(\mathrm{J})$	$\lvert C\rvert$	$\lvert S\rvert$	d_{s}	d_{k}	CPLEX	Gurobi
7	0	infeasible	—	—	—	—	89.1	417.3
7	−1	30.8941	30	7	1	0	93.5	1,096.9
7	−2	19.5696	31	7	2	0	107.9	12,521.6
6	0	infeasible	—	—	—	—	124.3	385.9
6	−1	30.8941	30	7	1	0	139.4	303.4
6	−2	14.6165	26	6	2	0	100.6	∗
5	0	infeasible	—	—	—	—	206.5	629.8
5	−1	1.0729	20	5	1	0	163.0	595.5
5	−2	1.0243	21	5	2	0	145.5	∗

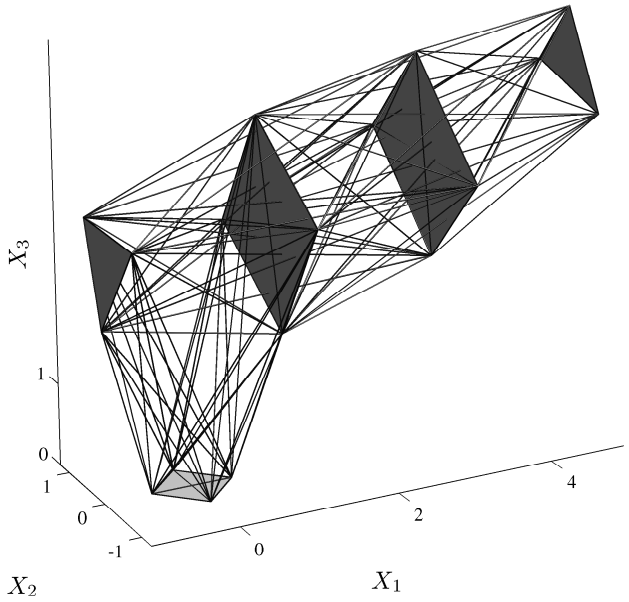

Figure 7: An L-shaped initial structure

solutions. It is evident from Table 2 that the solutions obtained by CPLEX in these two cases have smaller objective values than the solution for $(n^{\mathrm{s}}, n^{\mathrm{d}}) = (7, -2)$.

5.3. L-shaped tensegrity structure

In this section we consider an initial structure illustrated in Figure 7. This structure consists of $|V| = 18$ nodes and $|E| = 116$ members. The locations of the nodes are listed in Table 3. The nodes form five regular polygons, i.e., two equilateral triangles and three squares, as shown in Figure 7. We call the bottom square L_1. The remaining polygons are called $L_2, \ldots, L_5$, where the leftmost triangle is L_2 and the rightmost triangle is L_5. Squares L_1 and L_3 are parallel to the X_1X_2-plane and the X_2X_3-plane, respectively. The lengths of edges of L_1 are $\sqrt{2}/2\,\mathrm{m}$, those of L_2 and L_5 are $3\sqrt{3}/4\,\mathrm{m}$, and those of L_3 and L_4 are $5\sqrt{2}/4\,\mathrm{m}$.

The members connecting the pairs $\{L_1, L_4\}$, $\{L_1, L_5\}$, and $\{L_2, L_5\}$ are not considered. The number of pairs of intersecting members (with threshold $\delta = 0.05\,\mathrm{m}$) is $|P_{\mathrm{cross}}| = 53$.

Table 3: Locations of the nodes of the L-shaped initial structure in Figure 7

		L_1	L_2	L_3	L_4	L_5
Node 1	X_1	0.5000	−0.9749	1.0000	2.8682	4.9122
	X_2	0.0000	0.6495	1.2074	0.0000	0.7244
	X_3	0.0000	3.1993	2.6765	4.7682	4.1980
Node 2	X_1	0.0000	−1.0730	1.0000	2.9772	4.9706
	X_2	0.5000	0.0000	−0.3235	1.2500	−0.5303
	X_3	0.0000	2.0785	1.7926	3.5229	3.8669
Node 3	X_1	−0.5000	−0.9749	1.0000	3.0861	4.7527
	X_2	0.0000	−0.6495	−1.2074	0.0000	−0.1941
	X_3	0.0000	3.1993	3.3235	2.2777	5.1026
Node 4	X_1	0.0000		1.0000	2.9772	
	X_2	−0.5000		0.3235	−1.2500	
	X_3	0.0000		4.2074	3.5229	

Table 4: Computational results of the L-shaped example

						CPU (s)	
n^{d}	w (J)	$\lvert C\rvert$	$\lvert S\rvert$ $(= n^{\mathrm{s}})$	d_{s}	d_{k}	CPLEX	Gurobi
−1	infeasible	—	—	—	—	18,286.1	**
−2	6.3504	41	9	2	0	14,459.3	**
−3	9.6019	42	9	3	0	35,559.7	**

The equilibrium state under the self-weight load is considered by fixing all four nodes of L_1. Hence, $|J_{\mathrm{D}}| = 12$ and $|J_{\mathrm{N}}| = 42$. The lower bound for the number of struts is $n^{\mathrm{s}} = 9$. Then problem (4.18) has $2|E| = 232$ binary variables, $5|E| + 3|V| = 634$ continuous variables, 2276 linear inequality constraints, and 225 linear equality constraints.

The computational results are listed in Table 4. Here, the symbol "**" means that Gurobi Optimizer does not terminate within 100,000 s. The solutions obtained by CPLEX are shown in Figure 8. It is observed that sets of struts are different between Figures 8(a) and (b).

6. Conclusions

For developing real-world innovative tensegrity structures, form-finding methods that can explore diverse topologies are desired. In this paper we have explored a topology optimization problem of tensegrity structures subjected to self-weight loads. The presented approach prepares an initial structure with sufficiently large number of candidate members and does not require a topology of tensegrity structures to be known in advance. The optimization problem has been reduced to an MILP problem. It has been shown in numerical examples that various configurations of tensegrity structures can be obtained by solving this MILP problem. The numerical experiments illustrate that, for this MILP problem, Gurobi Optimizer is not superior to CPLEX from viewpoints of computational efficiency and accuracy.

This paper has not addressed issues of stability of tensegrity structures. The tensegrity

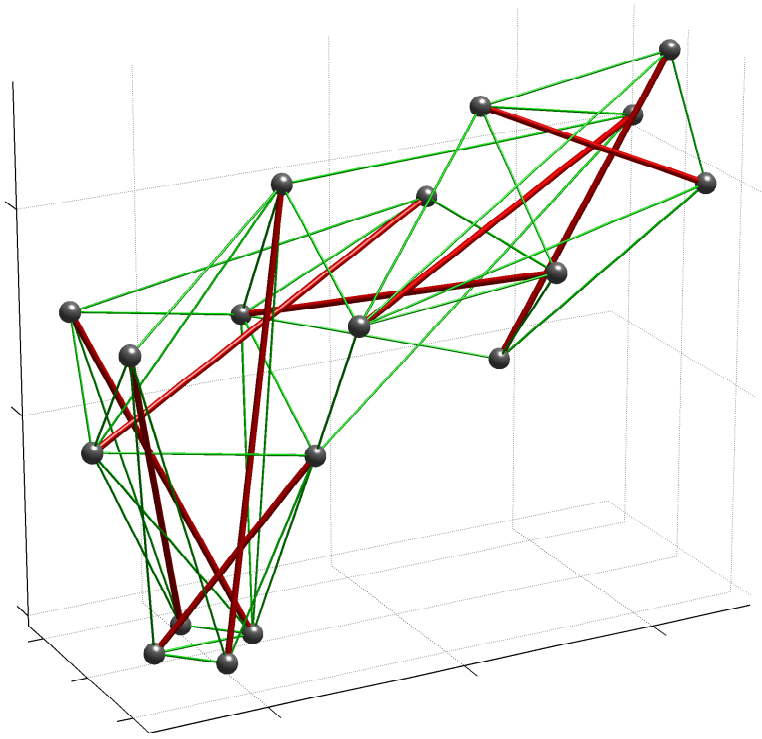

(a)

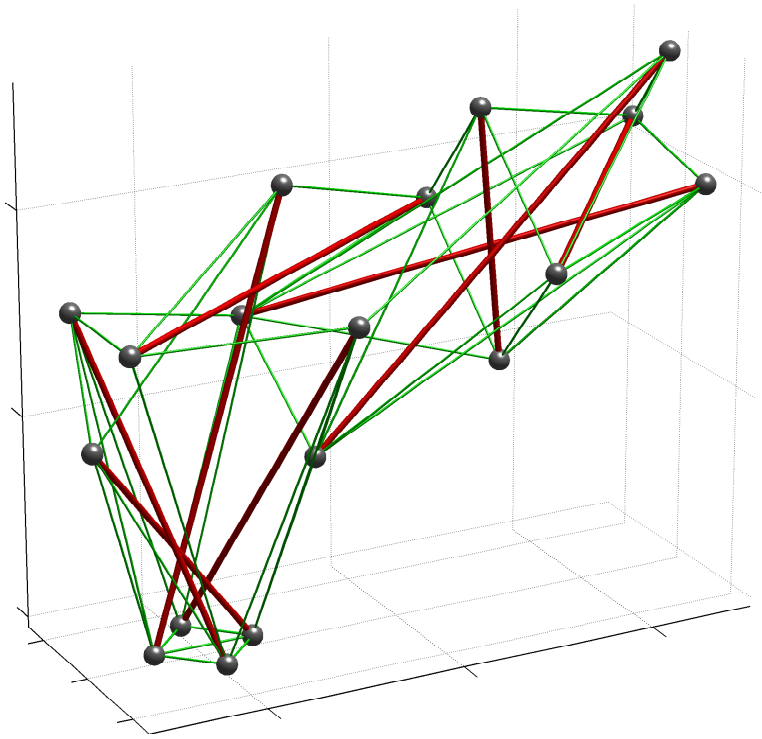

(b)

Figure 8: Optimal solutions obtained from the L-shaped initial structure in Figure 7. (a) $n^{\mathrm{d}} = -2$; (b) $n^{\mathrm{d}} = -3$

structures obtained in Section 5 are kinematically determinate (i.e., stable), whereas many well-known tensegrity structures are kinematically indeterminate (i.e., unstable) and stabilized by introducing prestress forces; see, e.g., Calladine [7], Guest [14], Hanaor and Liao [16], and Pellegrino [25]. Therefore, it remains as an important future subject to develop a numerical method that can find unstable (but prestress stable) tensegrity structures. Also, the geometrical nonlinearity has not been considered. Furthermore, the proposed formulation results in a large MILP problem, which might be a potential disadvantage for finding tensegrity structures consisting of a large number of members.

Acknowledgments

This work is partially supported by Grant-in-Aid for Scientific Research (C) 23560663, by the Global COE Program "The Research and Training Center for New Development in Mathematics," and by the Aihara Project, the FIRST program from JSPS, initiated by CSTP.

References

[1] B. Adam and I.F.C. Smith: Active tensegrity: a control framework for an adaptive civil-engineering structure. *Computers and Structures*, **86** (2008), 2215–2223.

[2] T.M. Atanackovic: Optimal shape of column with own weight: bi and single modal optimization. *Meccanica*, **41** (2006), 173–196.

[3] A. Back and R. Connelly: *Catalogue of Symmetric Tensegrities* (web page). `http://mathlab.cit.cornell.edu/visualization/tenseg/tenseg.html` (Accessed October 2011).

[4] N. Bel Hadj Ali, L. Rhode-Barbarigos, A.A. Pascual Albi, and I.F.C. Smith: Design optimization and dynamic analysis of a tensegrity-based footbridge. *Engineering Structures*, **32** (2010), 3650–3659.

[5] S. Bereg: On characterizations of rigid graphs in the plane using spanning trees. *Graphs and Combinatorics*, **25** (2009), 139–144.

[6] M. Bruyneel and P. Duysinx: Note on topology optimization of continuum structures including self-weight. *Structural and Multidisciplinary Optimization*, **29** (2005), 245–256.

[7] C.R. Calladine: Buckminster Fuller's "tensegrity" structures and Clerk Maxwell's rules for the construction of stiff frames. *International Journal of Solids and Structures*, **14** (1978), 161–172.

[8] R. Connelly and A. Back: Mathematics and tensegrity. *American Scientist*, **86** (1998), 142–151.

[9] R. Connelly and W. Whiteley: Second-order rigidity and prestress stability for tensegrity frameworks. *SIAM Journal on Discrete Mathematics*, **6** (1996), 453–491.

[10] S. Ehara and Y. Kanno: Topology design of tensegrity structures via mixed integer programming. *International Journal of Solids and Structures*, **47** (2010), 571–579.

[11] D.G. Emmerich: Construction de réseaux autotendants. French Patent No. 1,377,290, September 28, 1964.

[12] R.B. Fuller: Tensile-integrity structures. U.S. Patent No. 3,063,521, November 13, 1962.

[13] R.B. Fuller: *Synergetics: Explorations in the Geometry of Thinking* (Collier McMillian, London, 1975).

[14] S.D. Guest: The stiffness of tensegrity structures. *IMA Journal of Applied Mathematics*, **76** (2011), 57–66.

[15] Gurobi Optimization, Inc.: *Gurobi Optimizer Reference Manual*. `http://www.gurobi.com/` (2010).

[16] A. Hanaor and M.-K. Liao: Double-layer tensegrity grids: static load response. Part I: analytical study. *Journal of Structural Engineering (ASCE)*, **117** (1991), 1660–1674.

[17] IBM ILOG: *User's Manual for CPLEX*. `http://www.ilog.com/` (2010).

[18] M.H. Imam: Shape optimization of umbrella-shaped concrete shells subjected to self-weight as the dominant load. *Computers and Structures*, **69** (1998), 513–524.

[19] T. Jórdan, A. Recski, and Z. Szabadka: Rigid tensegrity labelings of graphs. *European Journal of Combinatorics*, **30** (2009), 1887–1895.

[20] S.H. Juan and J.M. Mirats Tur: Tensegrity frameworks: static analysis review. *Mechanism and Machine Theory*, **43** (2008), 859–881.

[21] Y. Kanno: Topology optimization of tensegrity structures under compliance constraint: a mixed integer linear programming approach. *Optimization and Engineering*, to appear.

[22] B.L. Karihaloo and S. Kanagasundaram: Optimum design of statically indeterminate beams under multiple loads. *Computers and Structures*, **26** (1987), 521–538.

[23] D.-Y. Kwak, J.-H. Jeong, J.-S. Cheon, and Y.-T. Im: Optimal design of composite hood with reinforcing ribs through stiffness analysis. *Composite Structures*, **38** (1997), 351–359.

[24] R. Motro: *Tensegrity* (Kogan Page Science, London, 2003).

[25] S. Pellegrino: A class of tensegrity domes. *International Journal of Space Structures*, **7** (1992), 127–142.

[26] J. Rieffel, F. Valero-Cuevasa, and H. Lipson: Automated discovery and optimization of large irregular tensegrity structures. *Computers and Structures*, **87** (2009), 368–379.

[27] G.I.N. Rozvany: Optimal plastic design: allowance for selfweight. *Journal of the Engineering Mechanics Division (ASCE)*, **103** (1977), 1165–1170.

[28] G.I.N. Rozvany, H. Nakanamura, and B.T. Kuhnell: Optimal archgrids: allowance for selfweight. *Computer Methods in Applied Mechanics and Engineering*, **24** (1980), 287–304.

[29] G.I.N. Rozvany, K.M. Yep, T.G. Ong, and B.L. Karihaloo: Optimal design of elastic beams under multiple design constraints. *International Journal of Solids and Structures*, **24** (1988), 331–349.

[30] K. Snelson: Continuous tension, discontinuous compression structures. U.S. Patent No. 3,169,611, February 16, 1965.

[31] K. Snelson: *Kenneth Snelson* (web page). `http://www.kennethsnelson.net/` (Accessed October 2011).

[32] A.M.C. So and Y. Ye: A semidefinite programming approach to tensegrity theory and realizability of graphs. *Proceedings of the 17th Annual ACM-SIAM Symposium on Discrete Algorithms (SODA 06)*, 766–775, Miami (2006).

[33] C. Sultan and R. Skelton: Deployment of tensegrity structures. *International Journal of Solids and Structures*, **40** (2003), 4637–4657.

[34] A.G. Tibert and S. Pellegrino: Deployable tensegrity reflectors for small satellites. *Journal of Spacecraft and Rockets (AIAA)*, **39** (2002), 701–709.

[35] A.G. Tibert and S. Pellegrino: Review of form-finding methods for tensegrity structures. *International Journal of Space Structures*, **18** (2003), 209–223.

[36] K.Yu. Volokh, O. Vilnay, and M. Belsky: Tensegrity architecture explains linear stiffening and predicts softening of living cells. *Journal of Biomechanics*, **33** (2000), 1543–1549.

[37] S. Wandling, P. Cañadas, and P. Chabrand: Towards a generalised tensegrity model describing the mechanical behaviour of the cytoskeleton structure. *Computer Methods in Biomechanics and Biomedical Engineering*, **6** (2003), 45–52.

[38] C.-M. Wang and G.I.N. Rozvany: On plane Prager-structures—II: nonparallel external loads and allowance for selfweight. *International Journal of Mechanical Sciences*, **25** (1983), 529–541.

Yoshihiro Kanno
Department of Mathematical Informatics
University of Tokyo
7-3-1 Hongo, Tokyo 113-8656, Japan
E-mail: kanno@mist.i.u-tokyo.ac.jp